Production and Characterization of Poly(ethylene glycol dimethacrylate-styrene-glycidyl methacrylate) Microbeads

S. SENEL,[1] H. CICEK,[2] A. TUNCEL[2]

[1]Chemistry Department, Hacettepe University, 06532, Ankara, Turkey

[2]Chemical Engineering Department, Hacettepe University, 06532, Ankara, Turkey

Received 20 November 1996; accepted 30 June 1997

ABSTRACT: Nonswellable and swellable poly(ethyleneglycol dimethacrylate)-based microbeads that could react directly with the biological molecules were produced by a suspension polymerization procedure. For this purpose, ethyleneglycol dimethacrylate (EGDMA) was copolymerized with glycidyl methacrylate (GMA) in an aqueous suspension medium. Benzoyl peroxide and poly(vinyl alcohol) were used as the initiator and the stabilizer, respectively. The copolymerization provided nonswellable, tranparent, and spherical copolymer microbeads in the size range of 100–300 μm. On the other hand, swellable copolymer microbeads in the aqueous medium were obtained by using toluene as a diluent in the same copolymerization recipe. In a separate group of polymerizations, styrene (St) monomer was also included within the monomer phase to regulate the hydrophobicity of resulting microbeads. Nonswellable and swellable poly(EGDMA-St-GMA) microbeads were obtained by changing the type and concentration of the ingredients within the monomer phase. The effects of glycidyl methacrylate, styrene, and toluene concentrations on the microbead yield, the average size, and the swellability of microbeads were investigated. In the second part of the study, the interaction of produced microbeads with a selected enzyme (i.e., chymotrypsin) was investigated. The most stable chymotrypsin immobilization was achieved with the swellable poly(EGDMA)-based microbeads including styrene. © 1998 John Wiley & Sons, Inc. J Appl Polym Sci **67:** 1319–1334, 1998

Key words: ethyleneglycoldimethacrylate; glycidylmethacrylate; suspension polymerization; enzyme immobilization; chymotrypsin

INTRODUCTION

Polymer beads are widely used as carrier matrices in various medical and biological applications, such as drug delivery systems, scintigraphic imaging, affinity chromatograpy, enzyme immobilization, and cell culturing.[1–5] Suspension polymerization is usually preferred for the synthesis of spherical polymeric carriers in the size range of 10–1000 μm.[6] In this process, the porous matrices may be obtained by using diluents as extensively studied for polystyrene, polymethymethacrylate, and polyacrylamide.[7–14] The type and concentration of diluent in the monomer phase and the extent of crosslinking control the porosity of the microbeads produced by this process. The surface chemistry of polymer microbeads is also an important factor that controls the interaction between the polymer matrix and the biological molecule. In some cases, special activation methods (i.e., cyanogen bromide, carbodiimide, or glutaraldehyde, etc.) are applied for covalent immobiliza-

Correspondence to: A. Tuncel.

Journal of Applied Polymer Science, Vol. 67, 1319–1334 (1998)
 CCC 0021-8995/98/071319-16

tion of biological molecules onto the surface of polymeric matrices.[15] As it is known, these methods can be utilized only for the matrix surfaces including certain functionalities (i.e., hydroxyl, carboxyl, amine, etc.). The activation process is an additional step in the binding of biological molecules, and most of the activation agents are strongly toxic materials. The experimental difficulties in the application of activation process, the undesired chemical interactions between active sites and biological molecules, and the reproducibility of activation reaction can be considered among the main disadvantages of the conventional procedures. Alternatively, without applying an activation step, the direct binding of biological molecules onto the matrix surface is possible for the polymeric materials including proper functional groups (i.e., aldehyde or epoxypropyl, etc.).[16,17]

The hydrogel matrices having swelling ability within the aqueous medium can be produced by the polymerization of ethylene glycol methacrylates and dimethacrylates.[18,19] The studies relating to these monomers have been mainly focused on the bulk polymerization method.[13,20–25] The results of kinetic experiments on the bulk polymerization indicated that swellable matrices were obtained when the polymerization of ethylene glycol monomethacrylates was conducted in the presence of dimethacrylate crosslinking agents while the homopolymerization of dimethacrylates provided nonswellable matrices.

In our previous studies, we produced swellable and nonswellable plain poly(ethyleneglycol-dimethacrylate) (poly(EGDMA)) or poly(EGDMA)-based microbeads including different functional groups (i.e., hydroxyl or carboxyl) on their surfaces.[26–28] But, these particles can be used as carrier matrices for the immobilization of biological agents by activation of the surface functional groups. In this study, we aimed to produce nonswellable and swellable poly(EGDMA)-based microbeads, which could react directly with the biological molecules for the covalent attachment of these molecules onto the polymeric surface. For this purpose, EGDMA was copolymerized with glycidyl methacrylate, (GMA) by applying a suspension polymerization procedure. Styrene and toluene were included in the polymerization recipe to regulate the hydrophobicity of resulting microbeads and to create porosity within the poly(EGDMA)-based matrix, respectively. In the second part, the interaction of produced microbeads with a selected enzyme (i.e., chymotrypsin) was investigated and some preliminary results relating to this interaction were presented.

EXPERIMENTAL

Materials

Ethyleneglycol dimethacrylate (EGDMA, Aldrich Chem. Co., Milwaukee, WI) was purified by passing through active alumina. Styrene (St, Yarpet AS, Turkey) was distilled under vacuum. Glycidyl methacrylate (GMA, Aldrich Chem. Co.) was used without further purification. Benzoyl peroxide (BPO, Aldrich Chem. Co.) and polyvinyl alcohol (PVA, 88% hydrolized, M_r: 96,000, Aldrich Chem. Co.) were utilized as the initiator and the stabilizer, respectively. Toluene (Merck AG, Germany) was included in the copolymerization recipe as a diluent without further purification. α-Chymotrypsin (Sigma Chem. Co., St. Louis, MO) was selected as the model enzyme to test the usability of produced microbeads as a carrier matrix in the enzyme immobilization studies. Benzoyl-L-tyrosine ethylester (BTEE, Sigma Chem. Co.) was utilized as a synthetic substrate to assay the activity of immobilized α-chymotrypsin.

Determination of Monomer Properties

The solubilities of monomer phase ingredients (i.e., EGDMA, St, GMA and toluene) in the dispersion medium (4 mg/mL aqueous PVA solution) were determined at 20°C. The experimental procedure used for the determination of GMA solubility may be defined as follows: 0.1 mL GMA was added into the dispersion medium (100 mL) and the resulting mixture was magnetically stirred at 20°C for 10 min. GMA addition (0.1 mL in each step) into the dispersion medium was repeated until the phase separation was detected by observing the presence of undissolved GMA droplets in the resulting mixture. GMA solubility was calculated by using the total volume of GMA added into the dispersion medium until the phase separation was observed. A similar procedure was also followed for the determination of the solubilities for other ingredients.

The surface tensions of monomer phase ingredients and dispersion medium were measured at 20°C, in Traube Stalagmometer by using pure water as the reference liquid.

Production of Microbeads

Two different recipes were used in the suspension polymerization experiments. The first one provided compact, nonporous, and nonswellable poly(EGDMA-*co*-GMA) or poly(EGDMA-St-GMA) microbeads. In a typical suspension polymerization, the dispersion medium was prepared by dissolving 0.2 g of PVA in 50 mL of distilled water. On the other hand, 0.08 g BPO was dissolved within the monomer phase comprised of 4 mL EGDMA, 2 mL St, and 2 mL GMA. This solution was then transferred into the dispersion medium contained in a magnetically stirred glass polymerization reactor which was in a thermostatic water bath. The suspension was sealed and stirred at 400 rpm, at room temperature for 15 min for complete mixing of the two phases. Then, the reactor temperature was raised and kept at 70°C for 2 h. At the end of this period, the temperature was increased to 88°C and the polymerization was completed after 2 h. The second type of recipe provided porous and swellable poly(EGDMA-*co*-GMA) and poly(EGDMA-St-GMA) microbeads. A similar suspension polymerization procedure was followed, except proper amount of toluene was added as a diluent into the monomer phase before mixing into the dispersion medium. A washing procedure was applied after polymerization to remove the diluent and any unreacted monomer from the product. The polymer microbeads were filtered and resuspended within ethyl alcohol. The new dispersion was stirred for about 2 h at room temperature and the microbeads were isolated by decanting the liquid part. Microbeads were washed twice with ethyl alcohol and then, three times with distilled-deionized water using the same procedure. In the suspension polymerization experiments, GMA, styrene, and toluene concentrations in the droplet phase, and the stirring rate were changed. The effect of these variations on the microbead yield, the average size and the swellability of produced microbeads were investigated.

Characterization of Microbeads

Microbead Yield

The washed polymer microbeads were dried in a vacuum oven at 50°C for 48 h before weighing. The microbead yield was determined by the following expression, where, W_p and W_m were the weight of dry microbeads (g) and the total weight of monomers initially charged to the reactor (g), respectively.

$$\text{Microbead yield} = (W_p/W_m) \times 100 \quad (1)$$

Size Distribution of Microbeads

The size distribution of polymer microbeads were determined by a screen analysis using standard Tyler sieve series (W.S. Tyler International Comp., USA). The microbeads were photographed in an optical microscope (Nikon, Japan) with 40× magnification to observe the size distribution and the particle morphology.

Swellability of Microbeads

To determine the swelling ratio of microbeads, 5 g of dry sample were put into a cylindirical tube. The apparent volume of the bed formed by the dry microbeads (V_d) was measured. Then, 50 mL of distilled-deionized water was added into the tube. The sealed tube was shaken on a rotator with 30 rpm rotating rate for 24 h. At the end of this period, the apparent volume of the bed formed by the swollen microbeads (V_s) was recorded. The equilibrium swelling ratio was calculated based on the following expression:

$$\text{Equilibrium swelling ratio} = ((V_s - V_d)/V_d) \times 100 \quad (2)$$

Morphology of Microbeads

To show the porous structure of the beads, the poly(EGDMA-St-GMA) microbeads produced with the toluene/monomer phase ratio of 12/8 were dried *in vacuo* at 40°C. The dried beads were coated with a thin layer of gold (about 100 Å thickness) *in vacuo* and the micrographs showing the surface structure of microbeads were obtained by a scanning electron microscope (JEOL, JEM 1200EX, Japan). To have the electron micrographs showing the internal structure, the gold-coated and mechanically broken microbead samples were also examined by the scanning electron microscope.

Binding of α-Chymotrypsin onto the Microbeads

Three types of microbeads with different properties were tried as carrier matrices for the immobilization of α-chymotrypsin. Nonswellable poly(EGDMA-*co*-GMA) microbeads and two types of swellable poly(EGDMA-St-GMA) microbeads

produced with different toluene concentrations were used in these experiments.

After washing of the selected microbeads by applying the procedure described above, the microbeads were dried *in vacuo* at 50°C for 48 h. Dry microbeads (0.1 g) were treated with the 10 mL of enzyme solution containing 0.4 mg/mL of α-chymotrypsin. The enzyme solution was prepared with borate buffer having a pH of 7.8. The treatment were performed at +4°C by stirring the medium with 60 rpm for 24 h. Before and after interaction with the microbeads, the absorbance of the enzyme solution was measured at 280 nm by a UV spectrophotometer (Schimadzu, Japan). The amount of bound enzyme onto the microbeads was determined by using the difference between initial and final absorbance values. α-Chymotrypsin-immobilized poly(EGDMA)-based microbeads were extensively washed with cold borate buffer. The absorbance values of washing solutions were also measured at the same wavelength to detect any enzyme leakage from the polymeric matrix. The microbead samples were washed five times by using 20 mL of borate buffer in each washing. However, no significant absorbance value (higher than 0.02) indicating an appreciable enzyme leakage from the polymeric matrix was recorded. The enzyme immobilized microbeads were stored at +4°C in borate buffer having a pH of 7.8.

Free and Immobilized Enzyme Experiments

A separate group of activity experiments were performed with free enzyme by changing the initial BTEE concentration between 15–400 μM for the determination of kinetic parameters. The enzyme concentration (i.e, previously determined in our studies) was fixed to 0.25 μg/mL. These batch runs were performed at 25°C, by 120 cpm shaking rate, in a 20 mL of reaction medium at a pH of 7.8 and including 5% ethanol and 95% borate buffer (by volume). The Michealis-Menten kinetic parameters of free enzyme were determined by applying linear regression on the Lineweaver-Burk plot. A standart procedure described in the literature was used for the determination of initial reaction rates with free and immobilized chymotrypsin.[29,30] Benzoyl-L-tyrosine ethylester (BTEE) was selected as a synthetic substrate and the hydrolysis of BTEE by free or immobilized α-chymotrypsin was followed by measuring the increase in the absorbance of the reaction medium in a UV spectrophotometer at a wavelength of 258 nm. The initial reaction rate (i.e., the initial hydrolysis rate of BTEE) was expressed in terms of μM BTEE/min and calculated by using the linear part of the absorbance–time curve obtained for the initial course of the reaction. Following expression was used for calculation of the initial reaction rate ($-r_{BTEE}$),[30] where $(dA/dt)_i$ is the derivative of linear part of the absorbance–time curve during the initial course of reaction, which was determined by a linear regression analysis between absorbance and time. A_o and A_f are initial and final absorbance values of the reaction medium, respectively, and S_o (μM) is the initial BTEE concentration.

$$-r_{BTEE} = \{(dA/dt)_i/(A_f - A_O)\} \times S_O \quad (3)$$

The stability of immobilized chymotrypsin were examined in batch mode. In these experiments, the initial BTEE concetration was fixed to 239.3 μM and 0.1 g of poly(EGDMA)-based microbeads carrying immobilized α-chymotrypsin were used. The activity experiments with enzyme immobilized microbeads were performed at 25°C, by 120 cpm shaking rate, in a 20 mL of reaction medium having a pH of 7.8 and including 5% ethanol and 95% borate buffer (by volume). The activity of enzyme immobilized microbeads was measured five times by performing one run per 24 h for each carrier. Each run was continued for 240 min, and after the run, the enzyme immobilized beads were extensively washed with cold borate buffer and were stored in the refrigerator at +4°C during the time period between the succesive runs.

RESULTS AND DISCUSSION

Properties of Selected Polymerizations

Biological agents (i.e., proteins, enzymes, or antibodies) can be attached directly onto the polymeric matrices including reactive epoxypropyl group.[17,31,32] Glycidyl methacrylate (i.e., epoxypropyl methacrylate) is a commonly used comonomer for the synthesis of these matrices.[31,32] In this study, a suspension polymerization procedure was developed for the synthesis of nonswellable and swellable poly(EGDMA-*co*-GMA) and poly(EGDMA-St-GMA) microbeads in the size range of 100–300 μm. Toluene was included in the polymerization recipe as a diluent in the synthesis of poly(EGDMA)-based swellable microbeads.

According to the mathematical model com-

monly used by different researchers, the average particle size in the suspension polymerization process is directly proportional with the vessel diameter, the volume ratio of the droplet phase to suspension medium, the viscosity of droplet phase and the interfacial tension between the two immiscible phases, and inversely proportional with the stirrer diameter, the stirring speed, the viscosity of suspension medium, and the stabilizer concentration.[33–35] The polymerization system investigated by this study included three different monomers and a diluent. The crosslinker (EGDMA) concentration in the droplet phase was also kept at resonably high levels. Therefore, the studied system was more complex relative to a typical suspension polymerization recipe including only one monomer and/or crosslinker. Due to this reason, we did not expect an exact agreement between the experimental results and model predictions on the particle size and we used the proposed model only to explain the general effects of process variables and to find the reasons of observed tendencies. In all polymerizations, we used the same reactor for all polymerizations with a temperature program and a stabilizer concentration determined by the preliminary experiments to achieve the polymerizations without coagulation and with nearly quantitative microbead yields. Therefore, vessel diameter, stirrer diameter, stabilizer concentration, and viscosity of suspension medium were kept constant in all experiments. Under these constant conditions, we changed the composition of monomer phase, diluent/total monomer volume ratio, and stirring rate. So, we tried to observe the effects of model variables related to the changed experimental conditions on the microbead yield, the average size, the size distribution, and the swellability of resultant microbeads. Therefore, we mainly focused on the volume ratio of droplet phase to suspension medium, interfacial tension between two immiscible phases, viscosity of the droplet phase, and stirring rate to explain the variations occurred in the average size of resultant microbeads.

Some selected physical properties of ingredients used in our polymerization system are given in Table I. The solubility parameter values were taken from the literature or calculated by using related equations.[36,37] The viscosities of the droplet phase components and the viscosities of droplet phases prepared with different compositions were determined in an Ostwald viscometer at 20°C. Of course, the initial viscosity of droplet phase at the polymerization conditions is one of the major variables controlling the average size. But, the initial polymerization temperature (i.e., 70°C) was a reasonably high value to measure the viscosities of monomeric compounds without taking the risk of polymerization during the measurement period. Then, we preferred to perform the viscosity measurements at 20°C. The measured viscosity values can give an idea about the relative magnitude of viscosity change in the droplet phase when the monomer composition is changed.

The interfacial tension was estimated by using the surface tensions of two immiscible phases according to the following expression.[38]

$$\sigma_{\mathrm{I}} = \sigma_{\mathrm{DP}} - \sigma_{\mathrm{CP}} \tag{4}$$

where, σ_{I}, σ_{DP}, and σ_{CP} are the interfacial tension, the surface tension of droplet phase, and the surface tension of the dispersion medium, respectively. The surface tension of droplet phase was estimated by the following expression.[38]

$$\sigma_{\mathrm{DP}} = \Sigma\, x_i \sigma_i \tag{5}$$

where x_i and σ_i are the mol fraction and the surface tension of any ingredient in the droplet phase. We used experimentally determined surface tensions of the ingredients to calculate the surface tension of the droplet phase. These values are given in Table II. The surface tensions of droplet phase ingredients were also calculated by the following expression.[38]

$$\sigma_i = ((P_i/R_{Di})(n_i^2 - 1)/(n_i^2 + 2))^4 \tag{6}$$

where, P_i, R_{Di}, and n_i were the parachor, the molar refraction, and the refractive index of component i, respectively. The related parameters and the calculated surface tensions of droplet phase ingredients are also given in Table II. The comparison of experimental values with the calculated ones indicated that the surface tension of each ingredient in the droplet phase could be estimated within about 10% accuracy by using eq. (6). This consistency also indicated that the parachor and the molar refraction values were estimated correctly. The surface tension of dispersion medium (i.e., aqueous PVA solution, 4 mg/mL) was also measured as 60.6 dyn/cm at 20°C. Although the calculated interfacial tension values based on the experimentally determined surface tensions of ingredients are not the exact values

Table I The Physical Properties of Ingredients Used in the Suspension Polymerization System

Ingredient	Mol. Weight (g/gmol)	Density (g/ml)	Viscosity[a] (cp)	Solubility Parameter $(cal/cm^3)^{1/2}$	Solubility in Dispersion Medium[b] (v/v)%
EGDMA	198.22	1.050	3.12	9.2[c]	<0.1
GMA	142.15	1.045	2.35	9.5[d]	2.1
Styrene	104.14	0.903	0.76	9.3[e]	<0.1
Toluene	92.13	0.866	0.59	8.3[e]	<0.1
Water	18.02	1.000	1.00	23.4[e]	—

[a] Measured in Ostwald viscometer at 20°C by using water as a reference liquid.
[b] Dispersion medium: 4 mg/mL aqueous PVA solution at 20°C.
[c] Calculated by using molar attraction constants given in ref. 36.
[d] Calculated by using Hildebrand expression in ref. 36.
[e] Taken from ref. 37.

at the polymerization temperature, they can represent the tendency showing the variation of interfacial tension by the droplet phase compositon in the polymerization conditions. With the help of the values in Tables I and II, the typical properties of studied suspension polymerization systems may be listed as follows: (1) GMA is the most polar monomeric ingredient in the droplet phase, while the diluent (i.e., toluene) is the most apolar one. The solubility parameters of all monomers (i.e., EGDMA, St, and GMA) are in the range of 9.2–9.5. Therefore, all the monomers are infinitely soluble within eachother and form a homogeneous solution when they are mixed at any ratio. (2) The solubility parameters of all monomers are reasonably smaller than that of water. All the monomers will be preferentially located in the droplet phase when a homogeneneous solution of these monomers is dispersed within the aqueous medium. This case eliminates the risk of monomer leakage from the organic phase to the aqueous medium during polymerization. This conclusion is also supported by the solubilities of monomer phase ingredients within the dispersion medium (Table I). As seen here, the solubilities of EGDMA, St in the dispersion medium are less than 0.1% (v/v). Only GMA has an appreciable solubility within the dispersion medium (i.e., 2.1%). However, this value also indicates that a significant GMA leakage from the organic phase to the dispersion medium does not occur during the polymerization. (3) The individual surface tension of toluene is reasonably different than that of all monomers. Therefore, an appreciable change in the interfacial tension is expected, when toluene is introduced into the polymerization recipe. This may cause a change in the average size even the other polymerization conditions are kept constant. (4) A similar case to (3) is also valid for the viscosities of droplet phase ingredients. Styrene and toluene have reasonably lower viscosities relative to those of EGDMA and GMA.

By considering these properties, different suspension polymerization recipes were established

Table II The Surface Tensions and Related Parameters of Ingredients Used in the Suspension Polymerization System

Ingredient	Parachor (P_i)[a]	Molar Refraction (R_{Di})[b]	Ref. Index (n_i)[c]	Surf. Tension $(\sigma_i, dyn \cdot cm^{-1})$[d]
EGDMA	453.8	50.52	1.4549	33.0 (35.3)
GMA	307.4	33.94	1.4494	37.4 (34.9)
Styrene	274.1	35.07	1.5460	34.0 (37.5)
Toluene	246.1	30.93	1.4968	30.5 (29.4)

[a] Calculated by using Sudgen's original parachor contribution values in ref. 38.
[b] Calculated by using atomic and structural contributions to molar refraction in ref. 38.
[c] Taken from the related supplier catalog.
[d] The surface tension values were measured at 20°C. The predicted surface tension values by eq. (6) were also given within the parentheses.

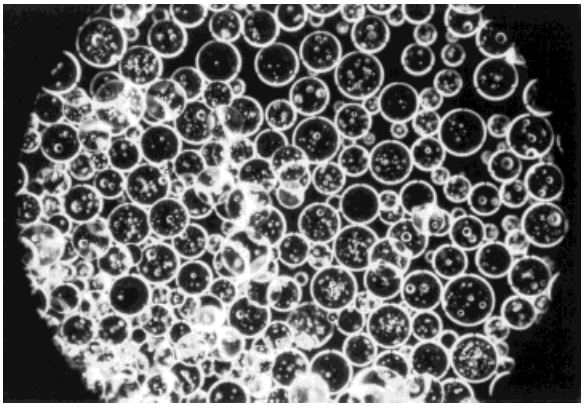

Figure 1 The optical micrograph of nonswellable poly(EGDMA-*co*-GMA) copolymer microbeads produced with 11.6% (by volume) GMA concentration within the monomer phase. Magnification: 40×.

for the production of nonswellable and swellable poly(EGDMA-*co*-GMA) and poly(EGDMA-St-GMA) microbeads.

Poly(EGDMA-*co*-GMA) Microbeads

In the first set of the copolymerization experiments, nonswellable poly(EGDMA-*co*-GMA) copolymer microbeads were produced by changing GMA concentration in the monomer phase between 0–33.4% (by volume), and by fixing droplet phase/suspension medium volumetric ratio to 6/50. BPO and PVA concentrations were 10 mg/mL based on total monomer and 4 mg/mL based on suspension medium, respectively. All polymerizations were performed with 400 rpm stirring rate by applying a temperature program described in the experimental section. A representative optical micrograph of poly(EGDMA-*co*-GMA) microbeads produced with the GMA concentration of 11.6% (by volume) is given in Figure 1. As seen here, transparent and nonporous poly(EGDMA-*co*-GMA) microbeads were obtained in the spherical form. No appreciable change was observed in the particle shape or morphology by the increasing GMA content within the monomer phase. The microbead yields with different GMA concentrations are given in Table III. As seen here, nearly quantitative monomer conversions to the microbead form could be achieved with all GMA concentrations. The microbead yields obtained with especially higher GMA concentrations clearly indicated that most of the GMA in the initial monomer mixture was succesfully incorporated into the resultant microbead structure and no significant coagulation occured in the studied conditions. The average size and the size distribution of copolymer microbeads are given in Table III and Figure 2, respectively. As seen in Figure 2, most of the microbeads (>50% based on weight) were collected in the size range of 210–250 μm for all batches. As seen in Table III, an increase in the GMA concentration caused a clear decrease in the droplet phase viscosity. A slight decrease was also observed in the interfacial tension, by the increasing GMA concentration. According to the common mathematical model of suspension polymerization, the decrease in the droplet phase viscosity or in the interfacial tension involves a decrease in the average size.[33–35] However, the magnitude of decrease observed experimentally was so small (i.e., the maximum average diameter difference in Table III was lower than 10%) to discuss the consistency between the mathematical model and the experimental results. It could be stated that GMA concentration was not as effective on the average particle size. On the other hand, no appreciable swelling was observed in the aqueous medium with the copolymer beads produced in this set.

Another copolymerization set was designed by including toluene as a diluent in the polymerization recipe. In this set, toluene/total monomer volumetric ratio was changed between 0/6–16/6 by fixing GMA/EGDMA volumetric ratio to 0.5. The other copolymerization conditions were the same with the those of the first set. The use of toluene as a diluent provided swellable copolymer microbeads in the aqueous medium. The optical micrographs of poly(EGDMA-*co*-GMA) copolymer microbeads produced with different toluene/monomer ratios are given in Figure 3. These micrographs were taken after the microbeads were swollen by distilled water. As seen here, the microbeads produced in this set were not transparent and the degree of opacity increased by the increasing toluene/monomer ratio. The increasing opacity may be an indicator for the increasing porosity of copolymer microbeads.[26–28] Swellable and spherical microbeads were achieved with the toluene/monomer ratios of 3/6 and 6/6 [Fig. 3(B) and (C)]. However, the broken microbeads were observed in the optical micrographs of the poly(EGDMA-*co*-GMA) samples produced with higher toluene concentrations [Fig. 3(D)]. The poor mechanical stability possibly originated from the increasing porosity by the increasing amount of toluene in the polymerization medium. The microbead yields and the equilibrium swelling ratios

Table III The Microbead Yields and Average Sizes of Nonswellable Poly(EGDMA-*co*-GMA) Microbeads with Different GMA Concentrations

C_{GMA} (% vol.)	MY (%)	DP/DM (mL/mL)	σ_{DP} (dyn · cm^{-1})	σ_I (dyn · cm^{-1})	μ (cp)	D (μm)
0 (0)[a]	91.0	0.12	33.0	27.6	3.12	234
11.6 (15.9)	91.2	0.12	33.7	26.9	2.96	224
20.0 (26.4)	96.5	0.12	34.2	26.4	2.90	221
33.3 (41.6)	95.5	0.12	34.8	25.8	2.82	216

Monomer phase: 6 ml, BPO: 60 mg.
C_{GMA}: GMA concentration within the monomer phase.
[a] The mol % of GMA in the monomer phase is given in the parenthesis. MY: Microbead yield, DP/DM: droplet phase/dispersion medium volumetric ratio; σ_{DP}: droplet phase surface tension; σ_I: surface tension difference between droplet phase and dispersion medium; μ: viscosity of droplet phase; D: average diameter of microbeads.

are given in Table IV. Satisfactory microbead yields were also obtained in the presence of toluene. As seen in Table IV, the copolymer microbeads having equilibrium swelling ratios varying from 30 to 60% within aqueous medium could be produced by increasing the amount of toluene.

The average size and the size distributions of swellable microbeads produced with different toluene concentrations are given in Table IV and Figure 4, respectively. Only, the size distributions of microbead samples produced with the toluene/monomer ratios of 3/6 and 6/6 were included in Figure 4, because the size analysis was not performed for the poly(EGDMA-*co*-GMA) microbeads including some broken particles (i.e., the batches produced with the toluene/monomer ratios of 12/6 and 16/6). As seen in Table IV, the average size of the microbeads slightly decreased with the toluene/monomer ratio of 3/6 relative to the recipe including no toluene. In the copolymerization including toluene/monomer ratio of 3/6, the droplet phase/dispersion medium ratio and the surface tension difference were higher relative to the the first recipe. Both of these factors involved an increase in the average size according to the empirical model of suspension polymerization.[33–35] But, the viscosity of droplet phase markedly decreased with the toluene/monomer ratio of 3/6 relative to the first recipe (i.e. from 2.82 to 1.54 cp). The decrease in the viscosity of droplet phase involved a decrease in the average size. Therefore, the compensation of size-increasing effects by the size-decreasing effect of viscosity change possibly prevented the formation of larger microbeads with the toluene/monomer ratio of 3/6, and roughly the same average sizes and size distributions were obtained with the first two recipes in this set. But, in the third run performed with the toluene/monomer ratio of 6/6, the average size clearly increased relative to the second copolymerization. Note that the droplet phase/dispersion medium ratio and the surface tension difference further increased by increasing the toluene/monomer ratio from 3/6 to 6/6. On the other hand, the decrease in the droplet phase viscosity (i.e., from 1.54 to 1.21) was reasonably smaller relative to the previous case. Therefore, the size-increasing effects of droplet phase/dispersion medium ratio and the interfacial tension may be dominant here, because a clear increase in the average size was observed with the toluene/monomer ratio of 6/6.

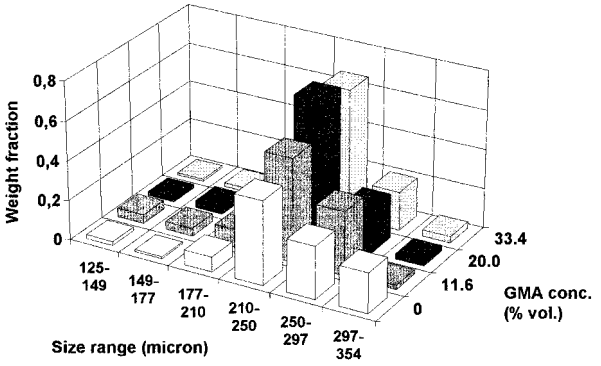

Figure 2 The size distributions of nonswellable poly(EGDMA-*co*-GMA) copolymer microbeads produced with different GMA concentrations.

Poly(EGDMA-St-GMA) Microbeads

Styrene was introduced into the suspension polymerization recipe to change the hydrophobicity of resultant microbeads because that was an important factor controlling the adsorption of biological molecules onto the polymer matrix. In this group of polymerizations, nonporous and nonswellable poly(EGDMA-St-GMA) microbeads

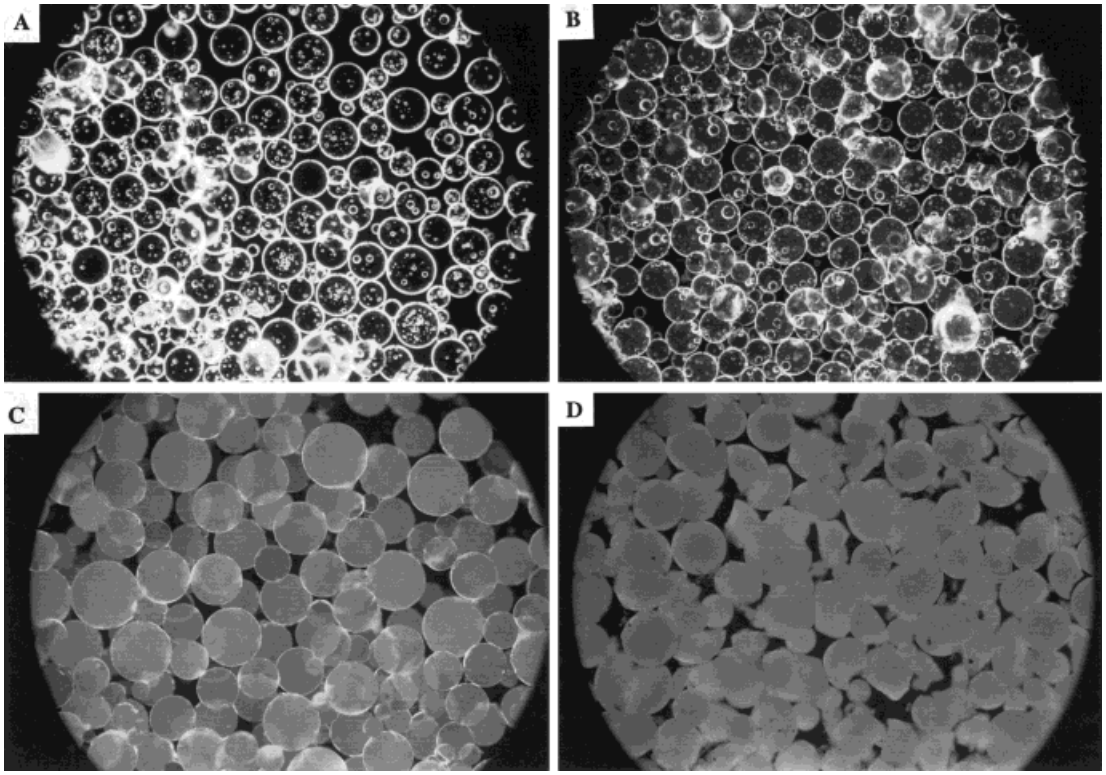

Figure 3 The optical micrographs of swellable poly(EGDMA-*co*-GMA) copolymer microbeads produced with different toluene/monomer ratios, Magnification: 40×. Toluene/monomer ratio (mL/mL): (A) 0/6, (B) 3/6, (C) 6/6, (D) 12/6.

were obtained by changing styrene concentration within the monomer phase between 0–25% by volume. Monomer phase/dispersion medium and GMA/EGDMA volumetric ratios were fixed to 8/50 and 0.5, respectively. BPO and PVA concentrations were 10 mg/mL based on total monomer and 4 mg/mL based on suspension medium, respectively. All polymerizations were performed with 400 rpm stirring rate by applying the temperature program described in the experimental section. The representative optical micrographs of poly(EGDMA-St-GMA) microbeads produced with different styrene concentrations are given in Figure 5. Transparent and nonswellable microbeads were obtained in the spherical form with all styrene concentrations. The average sizes and the

Table IV The Microbead Yields, Equilibrium Swelling Ratios, and Average Sizes of Swellable Poly(EGDMA-*co*-GMA) Microbeads

T/M (mL/mL)	MY (%)	ESR (%)	DP/DM (mL/mL)	σ_{DP} (dyn·cm^{-1})	σ_I (dyn·cm^{-1})	μ (cp)	D (μm)
0/6	95.5	ns	0.12	34.8	25.8	2.82	216
3/6	92.4	31.3	0.18	32.9	27.7	1.54	207
6/6	86.4	42.1	0.24	32.2	28.4	1.21	284
12/6	94.5	50.0	0.36	31.6	29.0	0.95	bm
16/6	95.3	63.6	0.44	31.3	29.3	0.88	bm

Monomer phase: 6 mL, GMA/EGDMA volumetric ratio: 0.5 mL/mL, BPO: 60 mg.

T/M: Toluene/total monomer volumetric ratio, MY: Microbead yield, ESR: Equilibrium swelling ratio of the microbeads within aqueous medium, DP/DM: Droplet phase/dispersion medium volumetric ratio, σ_{DP}: droplet phase surface tension, σ_I: surface tension difference between droplet phase and dispersion medium, μ: viscosity of droplet phase, D: average diameter of microbeads, ns: nonswellable microbeads, bm: some microbeads are in the broken form within the batch.

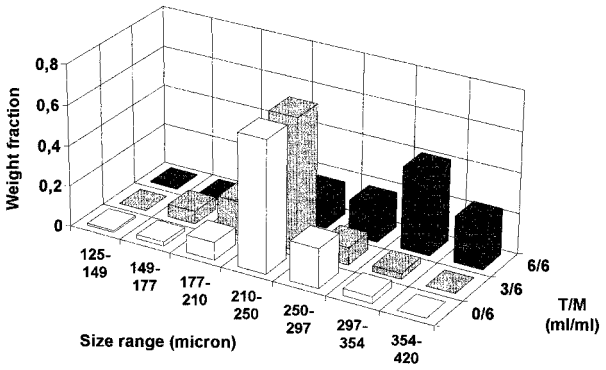

Figure 4 The size distribution of swellable poly(EGDMA-*co*-GMA) microbeads produced with different toluene/monomer ratios.

size distributions of these microbeads are given in Table V and Figure 6, respectively. As seen in Figure 6, roughly 70% of the beads were collected in the range of 297–354 μm when the styrene concentration was fixed to 25%, while about the same percent was in the range of 210–297 μm for the microbeads produced in the absence of styrene. The results indicated that the fraction of larger sizes and then the average size increased with the increasing styrene concentration. As seen in Table V, the viscosity of droplet phase decreased and the interfacial tension did not change with the increasing styrene concentration. The change in droplet phase viscosity involves a decrease in the average size according to the proposed model.[33–35] However, the observed tendency with the increasing styrene concentration was not consistent with the model. Note that the average size values with 14.4 and 25.0% of styrene concentrations were very close to each other. Both of these sizes were around 300 μm, and this value was roughly the highest average size in all polymerizations performed with 400 rpm stirring rate. Due to this observation, it may be a limited value possibly controlled by the used stirring rate.

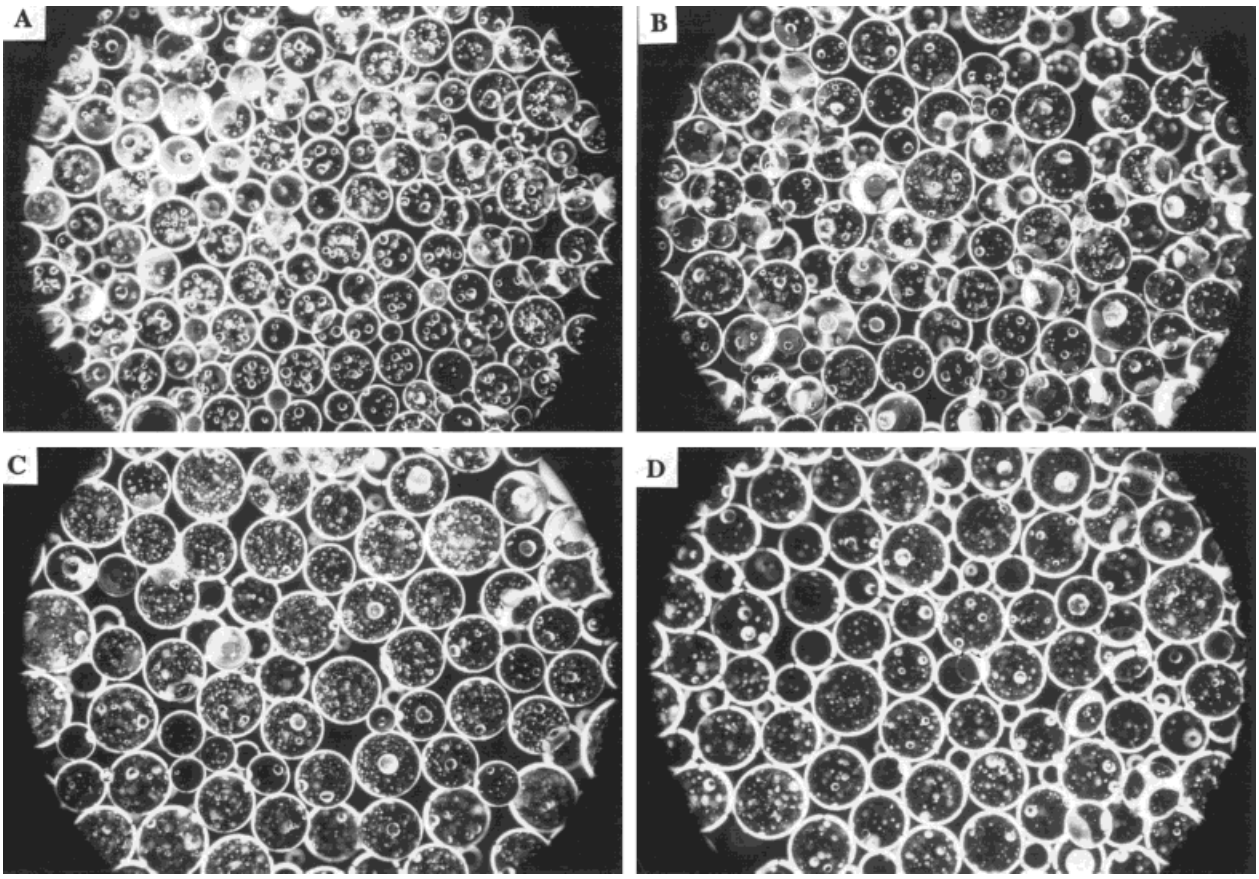

Figure 5 The representative optical micrographs of nonswellable poly(EGDMA-St-GMA) microbeads produced with different styrene concentrations, Magnification: 40×. Styrene concentration within the monomer phase (% volume): (A) 0, (B) 7.5, (C) 14.4, (D) 25.0.

Table V The Microbead Yields and Average Sizes of Nonswellable Poly(EGDMA-*St*-GMA) Microbeads with Different Styrene Concentrations

C_{St} (% vol.)	MY (%)	DP/DM (mL/mL)	σ_{DP} (dyn · cm^{-1})	σ_I (dyn · cm^{-1})	μ (cp)	D (μm)
0 (0)[a]	95.5	0.16	34.8	25.8	2.82	233
7.5 (10.4)	89.5	0.16	34.7	25.9	2.46	264
14.4 (19.4)	92.5	0.16	34.6	26.0	2.23	309
25.0 (32.3)	94.6	0.16	34.6	26.0	1.97	292

Monomer phase: 8 mL, GMA/EGDMA volumetric ratio: 0.5 mL/mL (0.71 mol/mol), BPO: 80 mg.
C_{St}: St concentration within the monomer phase.
[a] The mol % of St in the monomer phase is given in the parentheses. MY: microbead yield; DP/DM: droplet phase/dispersion medium volumetric ratio; σ_{DP}: droplet phase surface tension; σ_I: surface tension difference between droplet phase and dispersion medium; μ: viscosity of droplet phase; D: average diameter of microbeads.

Therefore, the size increasing effect of styrene was possibly suppressed by the stirring rate in the polymerization performed with 25% styrene concentration and the applied mechanical breaking effect on the droplet phase (i.e., the used stirring rate) did not allow a further size increase above 300 μm in the studied system. The microbead yields of nonswellable poly(EGDMA-St-GMA) particles with different styrene concentrations are given in Table V. The microbead yields with higher styrene concentrations clearly indicated the introduction of styrene into the microbead structure.

The swellable form of poly(EGDMA-St-GMA) microbeads were obtained by introducing toluene into the suspension polymerization recipe. In these experiments, toluene/monomer phase ratio was changed between 0/8–16/8 by fixing St/EGDMA and GMA/EGDMA volumetric ratios to 0.5. The other polymerization conditions were the same with the those used in the production of nonswellable poly(EGDMA-St-GMA) microbeads.

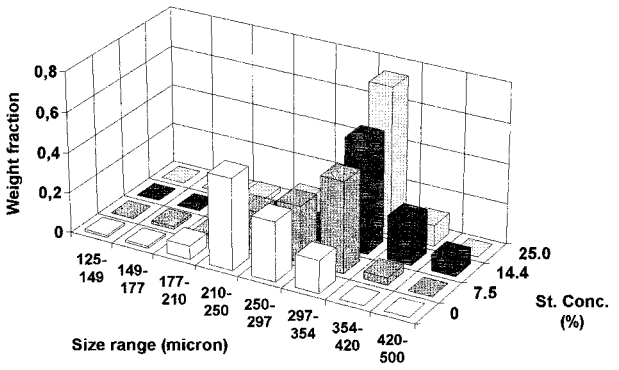

Figure 6 The size distribution of nonswellable poly(EGDMA-St-GMA) microbeads produced with different styrene concentrations.

The representative optical micrographs of swellable poly(EGDMA-St-GMA) microbeads are given in Figure 7. As seen here, these microbeads were obtained in the opaque form and the degree of opacity increased by the increasing toluene concentration. Note that a significant amount of broken particles was observed within the swellable poly(EGDMA-*co*-GMA) microbeads produced with higher toluene concentrations [Fig. 3(D)]. However, the presence of broken particles was not detected in the optical microscope examinations performed with the swellable poly(EGDMA-St-GMA) particles produced with reasonably similar conditions [Fig. 7(C) and (D)]. This result indicated that the introduction of styrene into the polymerization recipe increased the mechanical stability of microbeads produced with higher toluene concentrations. The average sizes and the size distributions of swellable poly(EGDMA-St-GMA) particles produced with different toluene concentrations are given in Table VI and Figure 8, respectively. The variation of average size with the increasing toluene concentration was reasonably similar to that observed with the swellable poly(EGDMA-*co*-GMA) microbeads. The average size was lower with a toluene/monomer ratio of 6/8 relative to the recipe including no toluene. Note that a marked decrease in the viscosity of droplet phase (i.e., from 1.97 to 1.12) occurred when the toluene/monomer ratio of 6/8 was used. The size decreasing effect of this change was possibly dominant relative to the size increasing effects of interfacial tension and droplet phase/dispersion medium ratio in the copolymerization performed with 6/8 toluene/monomer ratio. After 6/8 toluene/monomer ratio, the droplet phase viscosity decreased more slowly, and droplet phase/dispersion medium ratio and interfacial tension

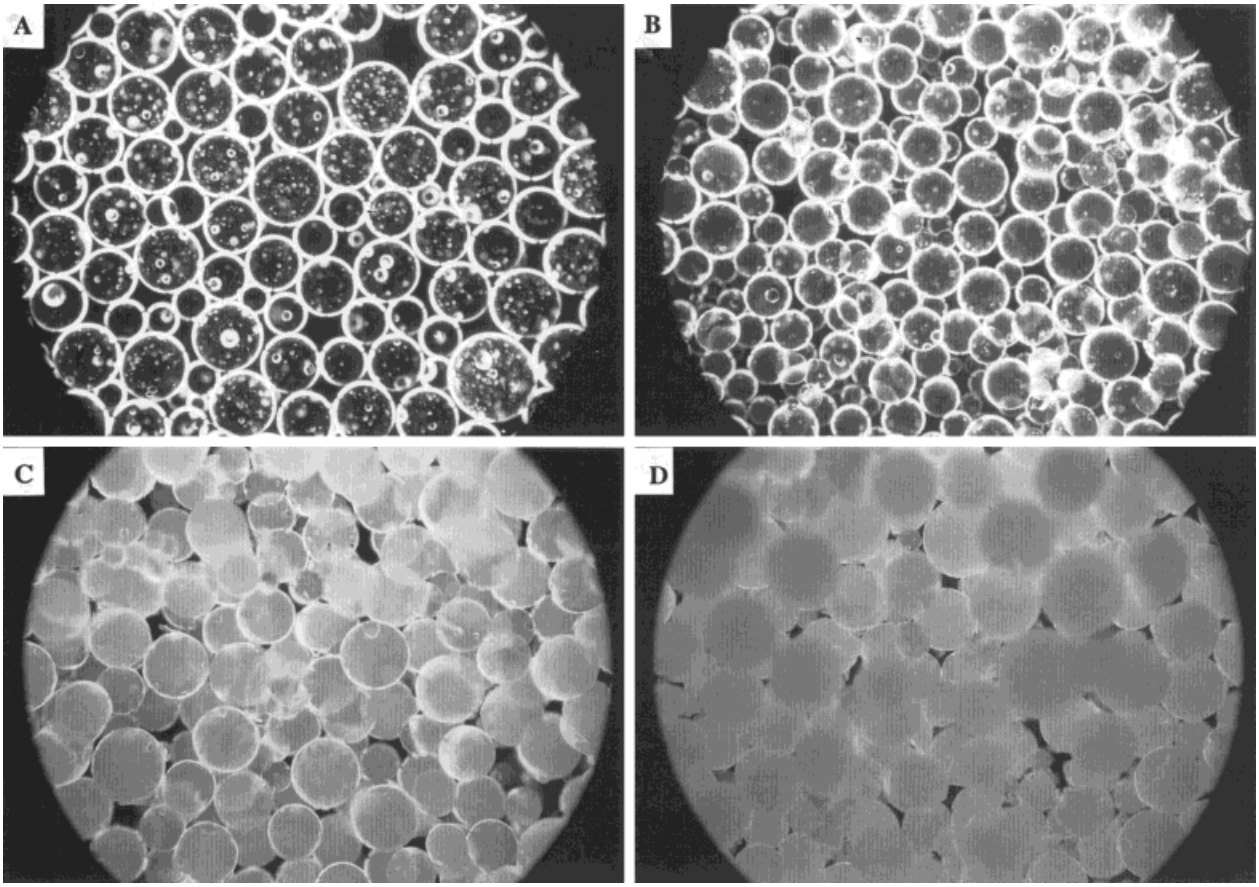

Figure 7 The representative optical micrographs of swellable poly(EGDMA-St-GMA) microbeads. Magnification: 40×. Toluene/monomer ratio (mL/mL): (A) 0/8, (B) 6/8, (C) 12/8, (D) 16/8.

increased markedly with the increasing toluene concentration. Therefore, an appreciable increase in the average size was obtained by the increasing toluene/monomer ratio. Note that the highest average is in this set was also around 300 μm.

The equilibrium swelling ratios of the swellable poly(EGDMA-St-GMA) microbeads in the aqueous medium are given in Table VI. The equilibrium swelling ratio increased by increasing toluene concentration, as was expected. On the other

Table VI The Microbead Yields, Equilibrium Swelling Ratios, and Average Sizes of Swellable Poly(EGDMA-*St*-GMA) Microbeads

T/M (mL/mL)	MY (%)	ESR (%)	DP/DM (mL/mL)	σ_{DP} (dyn·cm^{-1})	σ_I (dyn·cm^{-1})	μ (cp)	D (μm)
0/8	94.6	ns	0.16	34.6	26.0	1.97	292
6/8	95.7	12.5	0.28	32.5	28.1	1.12	242
12/8	93.8	14.3	0.40	31.9	28.7	0.94	288
16/8	91.7	17.1	0.48	31.6	29.0	0.83	318

Monomer phase: 8 mL, EGDMA: 4 mL, GMA: 2 mL, Styrene: 2 mL, BPO: 80 mg.

T/M: Toluene/total monomer volumetric ratio; MY: microbead yield; ESR: equilibrium swelling ratio of the microbeads within aqueous medium; DP/DM: droplet phase/dispersion medium volumetric ratio; σ_{DP}: droplet phase surface tension, σ_I: surface tension difference between droplet phase and dispersion medium μ: viscosity of droplet phase; D: average diameter of microbeads; ns: nonswellable microbeads.

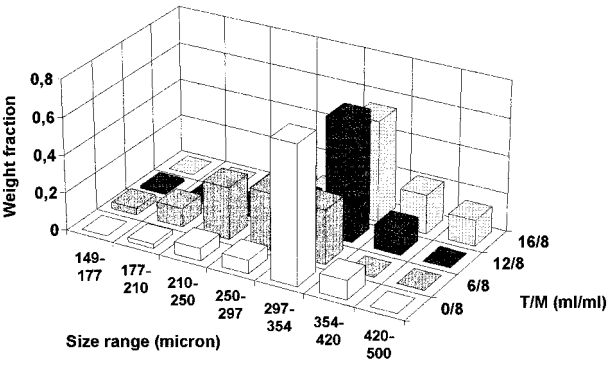

Figure 8 The size distributions of swellable poly(EGDMA-St-GMA) microbeads produced with different toluene/monomer ratios.

hand, the equilibrium swelling ratios of poly(EGDMA-St-GMA) microbeads were significanty lower relative to those obtained with the poly(EGDMA-*co*-GMA) microbeads (Table IV) due to the introduction of styrene monomer. It can be concluded that the hydrophilicity of poly(EGDMA-St-GMA) microbeads is lower than that of poly(EGDMA-*co*-GMA) structure.

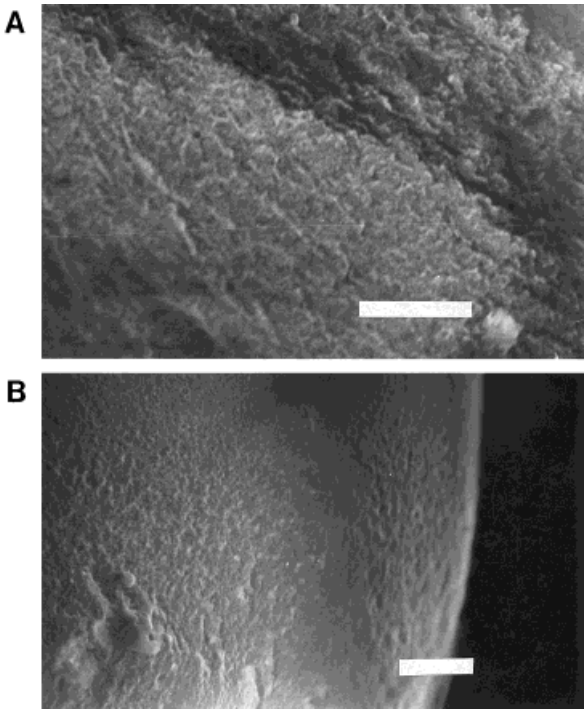

Figure 9 The electron micrographs showing the morphology of swellable poly(EGDMA-St-GMA) microbeads: (A) the internal structure of the mechanically broken microbeads, (B) the surface structure of dry microbeads. The bars in the SEM photographs indicate 10 μm.

Table VII The Microbead Yields and Average Sizes of Swellable Poly(EGDMA-*St*-GMA) Microbeads with Different Stirring Rates

Stirring Rate (rpm)	Microbead Yield (%)	Average Size (μm)	Type of Particle Size Distribution
200	95.1	320	bimodal
400	95.7	242	broad monomodal
1000	96.2	122	bimodal

EGDMA: 4 mL, Styrene: 2 mL, GMA: 2 mL, Toluene: 6 mL, BPO: 80 mg.

The internal and surface structures of the swellable poly(EGDMA-St-GMA) particles were exemplified in Figure 9(A) and (B), respectively. These micrographs were taken with the dry poly(EGDMA-St-GMA) particles produced by the toluene/monomer ratio of 12/8. As seen in Table VI, the selected sample exhibited a reasonably low equilibrium swelling ratio (i.e., 14.3%) in the aqueous medium. For this reason, the porosity of dry particles should be reasonably close to the porosity of swollen polymeric matrix. Therefore, the SEM photographs of dry particles can give an idea about the morphology of swollen particles. As seen in Figure 9(A), taken with the mechanically broken particle sample, the examined bead had a porous interior. It was possible to see micron-size pores (i.e., large pores) within the internal structure dominantly contained reasonably small pores in the submicron size range. This result indicated that the pore size distribution was not narrow within the internal structure. However, as seen in Figure 9(B), the pore size distribution was narrower on the bead surface contained the pores in the submicron size range.

As reported in the literature, the stirring rate is one of the important parameters controlling average size and size distribution of microbeads in the suspension polymerization process.[33–35] The effect of stirring rate on the size distribution of poly(EGDMA-St-GMA) microbeads was studied by changing this variable between 200–1000 rpm. In these experiments, monomer/dispersion medium volumetric ratio was 8/50. St/EGDMA and GMA/EGDMA volumetric ratios were fixed to 0.5. Toluene was also included in the polymerization recipe and the toluene/monomer volumetric ratio was fixed to 6/8. BPO and PVA concentrations were 10 mg/mL monomer and 4 mg/mL, respectively. The same temperature program with the other polymerizations was applied. No significant

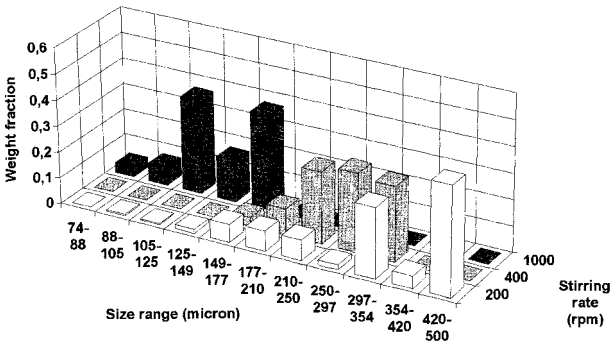

Figure 10 The size distributions of swellable poly(EGDMA-St-GMA) microbeads produced with different stirring rates.

effect of stirring rate on the microbead yield was observed, as given in Table VII. The variation of average size and the variation of size distribution of swellable poly(EGDMA-St-GMA) microbeads with the stirring rate are given in Table VII and Figure 10, respectively. The increase in the stirring rate caused a significant decrease in the average size, as it was expected.[33–35] As seen in Figure 10, the largest average particle size was obtained with 200 rpm stirring rate. However, the particles were mainly collected in the two size ranges, which were 297–354 and 420–500 μm. Therefore, the bimodal character was dominant in the particle size distribution. A similar property was also observed in the particle size distribution with the highest stirring rate (i.e., 1000 rpm). Note that the smallest average size was achieved with this size distribution. On the other hand, a broad monomodal size distribution between 149–354 μm were obtained with 400 rpm stirring rate. The optical micrographs of the microbeads produced with the lowest and highest stirring rates are given in Figure 11. As seen here, the stirring rate was the most important parameter controlling the average size and size distribution in this polymerization system.

α-Chymotrypsin Immobilization

α-Chymotrypsin was used as the model enzyme only to show the usability of produced beads in the immobilization studies. To test the consistency of Michealis-Menten kinetics for free enzyme, the inital BTEE concentration was changed between 15–400 μM. The batch runs were performed at 25°C and at a pH of 7.8 by using a 0.005 mg enzyme within 20 mL of the reaction volume (i.e., the enzyme concentration was 2.5×10^{-4} mg/mL). K_m and r_m values for free enzymes were found as 63 μM and 11.0 μM/min by using the Lineweaver-Burk plot.

The selected enzyme was immobilized onto three different poly(EGDMA)-based microbeads containing GMA. The production conditions and the enzyme binding capacities of these microbeads are given in Table VIII. As seen here, the lowest enzyme binding (i.e., 0.83 mg CT/g beads) was obtained with the nonswellable and nonporous poly(EGDMA-*co*-GMA) microbeads. However, resonably higher enzyme binding capacities (up to 23.20 mg CT/g beads) could be achieved with the swellable poly(EGDMA-St-GMA) microbeads. It should be noted that these beads had a porous interior because they were produced by using toluene as the diluent in the polymerization (Fig. 9). For poly(EGDMA-St-GMA) microbeads, the available surface area for enzyme binding was resonably higher relative to the nonporous and nonswellable poly(EGDMA-*co*-GMA) microbeads. As also seen in Table VIII, the increase in the toluene/monomer ratio during

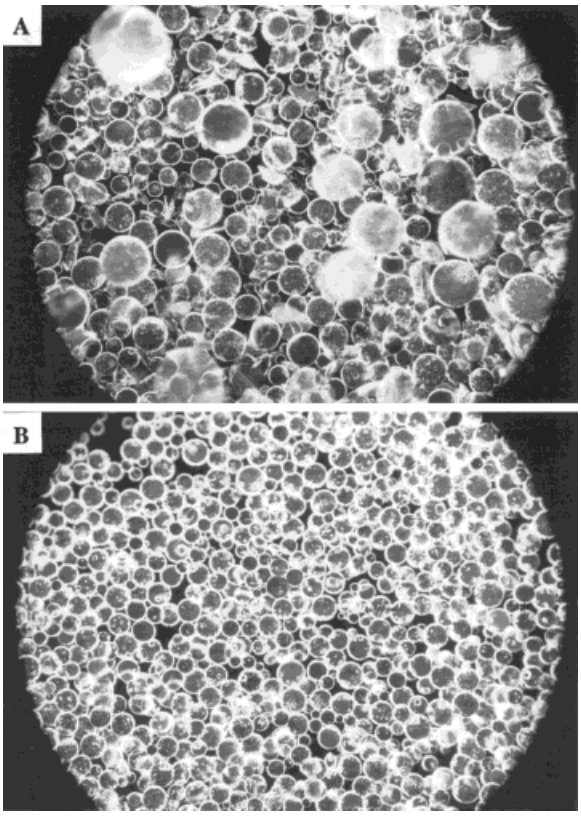

Figure 11 Representative optical micrographs of swellable poly(EGDMA-St-GMA) microbeads produced with different stirring rates. Magnification: 40×. Stirring rate (rpm): (A) 200, (B) 1000.

Table VIII The Kinetic Behavior of α-Chymotrypsin Carrying Poly(EGDMA)-Based Microbeads

Carrier Type	Enzyme Binding Capacity (mg CT/g bead)	Amount of Enzyme Used in One Batch (mg CT)	Apparent Reaction Rate (μM BTEE/min)	Carrier Activity (μmol BTEE/ mg CT-min)
Free enzyme	—	0.005	11.0	44.00
Nonswellable poly(EGDMA-*co*-GMA) (no toluene)	0.83	0.083	2.75	0.663
Swellable poly(EGDMA-*St*-GMA) (toluene/monomer: 6/8)	4.99	0.499	3.75	0.151
Swellable poly(EDGMA-*St*-GMA) (toluene/monomer: 12/8)	23.20	2.320	4.10	0.035

EGDMA: 4 mL, Styrene: 2 mL or [a]none, GMA: 2 mL, BPO: 10 mg/mL.
[a] No styrene was used in the preparation of nonswellable Poly(EGDMA-*co*-GMA) microbeads.

the polymerization resulted in a significant increase in the enzyme binding capacity of poly(EGDMA-St-GMA) microbeads. This increase may also be explained by the higher porosity of microbeads produced by using higher amount of diluent in the polymerization.

The apparent reaction rates with the α-chymotrypsin immobilized poly(EGDMA)-based microbeads were measured by fixing the initial BTEE concentration to 239.3 *μM*. In these runs performed by using 0.1 g of α-chymotrypsin immobilized microbeads within 20 mL of reaction volume, the temperature and pH were 25°C and 7.8, respectively. The reaction rate in the presence of free enzyme was also determined in the same conditions by using 0.005 mg α-chymotrypsin within the same reaction volume. The apparent reaction rates with α-chymotrypsin immobilized poly(EGDMA)-based microbeads are given in Table VIII. Here, the apparent reaction rate was defined as μmole BTEE consumed per minute per unit reaction volume. As seen in Table VIII, the reaction rates changing between 20 and 50% of that observed with the free enzyme, could be achieved with 0.1 g of microbeads carrying different amounts of immobilized enzyme.

On the other hand, higher apparent reaction rate was obtained with the microbeads having higher enzyme content. However, the increase in the apparent reaction rate was not proportional to the increase in the enzyme content. To discuss this result, the enzymatic activities of the produced microbeads based on the loaded enzyme were determined (Table VIII). Here, the carrier activity was defined as the amount of subtrate converted per unit time by per mg of immobilized enzyme. A similar definition was also made for the free enzyme. The results indicated that the carrier activities were reasonably low relative to that of free enzyme. On the other hand, the carrier activity significantly decreased with the increasing enzyme binding capacity. This result may be explained as follows: first, a significant part of the enzyme bound to the polymeric matrix is in the inactive form. The conformational changes occurred in the enzyme molecules during the binding process or the binding of enzyme molecules to the polymeric matrix via their active sites against the substrate molecules lead to a decrease in the activity of the carrier matrix. Second, the internal mass transfer resistance against the substrate diffusion may be the another reason for the activity decrease observed for swellable porous matrices.

To test the stability of immobilized α-chymotrypsin a series of batch runs were performed with the each matrix by fixing initial BTEE concentration to 239.3 *μM*. The conditions of these runs were the same with the first run described above. The variation of apparent reaction rate with the run number is given in Figure 12 for all microbeads carrying immobilized enzyme. As seen here, a drastic decrease in the apparent reaction rate was observed after the first run for all matrices. This case possibly originated from the leakage of weakly bound enzyme molecules from the polymeric matrix. The decrease in the enzymatic activity after the second run remained within the acceptible limits and slightly decreasing, but appreciable activities could be obtained with especially swellable and styrene containing poly(EGDMA)-based microbeads.

It should be noted that the preliminary results relating to the enzyme binding are presented here

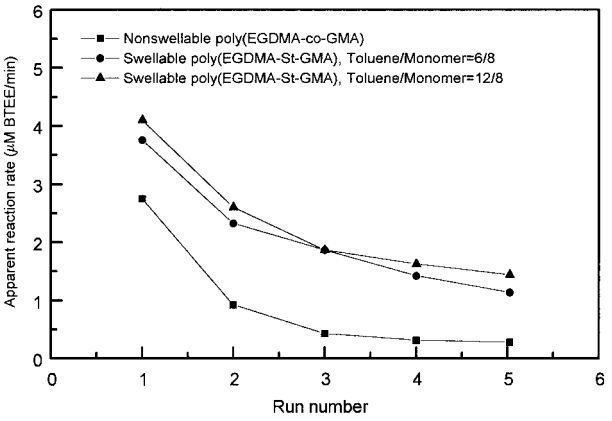

Figure 12 The variation of apparent reaction rate with the run number for α-chymotrypsin carrying poly-(EGDMA)-based matrices.

and the interaction of different enzymes (i.e., chymotrypsin and lipase) with the produced microbeads, the optimization of binding conditions, and the kinetic behaviors of immobilized enzymes are still under investigation.

REFERENCES

1. J. Woodward, Ed., *Immobilized Cells and Enzymes: A Practical Approach,* IRL Press, Oxford, 1985.
2. A. Rembaum and Z. A. Toke, Eds., *Beads: Medical and Biological Applications,* CRC Press, Boca Raton, FL, 1988.
3. D. S. Kompala and P. Todd, Eds., *Cell Separation Science and Technology,* ACS Symposium Series 464, American Chemical Society, Washington, DC, 1991.
4. R. Arshady, *Biomaterials,* **14,** 5 (1993).
5. G. Subramanian, B. A. Rhodes, J. F. Cooper, and V. J. Sodd, Eds., *Radiopharmaceuticals,* Society of Nuclear Medicine, New York, 1975.
6. R. Arshady, *Colloid Polym. Sci.,* **270,** 717 (1992).
7. J. Seidel, J. Malinsky, K. Dusek, and W. Heitz, *Adv. Polym. Sci., Polym. Symp.,* **42,** 835 (1973).
8. W. Heitz, *Adv. Polym. Sci.,* **23,** 1 (1977).
9. D. Horak, Z. Pelzbauer, M. Bleha, M. Havsky, F. Svec, and J. Kalal, *J. Appl. Polym. Sci.,* **26,** 109 (1990).
10. D. Horak, F. Svec, M. Bleha, and J. Kalal, *Angew. Makromol. Chem.,* **95,** 109 (1981).
11. P. P. Wieczorek, M. Ilavky, B. N. Kolarz, and K. Dusek, *J. Appl. Polym. Sci.,* **27,** 297 (1982).
12. Y. Ohtsuka, H. Kawaguchi, and Y. Yamamoto, *J. Appl. Polym. Sci.,* **27,** 3279 (1982).
13. H. Galina, N. B. Colaz, P. P. Wiezorek, and M. Woiszynska, *Br. Polym.,* **17,** 215 (1985).
14. M. Dimonie, H. D. Schell, G. Hubcka, M. A. Mateescu, C. G. Oprescu, S. Todireanu, O. Maior, J. Languri, and M. Iosif, *J. Macromol. Sci.-Chem.,* **A22,** 729 (1985).
15. *Affinity Chromatography: Principles and Methods,* Pharmacia Fine Chemicals Publications, Uppsala, 1979.
16. S. Margel and E. Wiesel, *J. Polym. Sci., Polym. Chem. Ed., Part A,* **22,** 145 (1984).
17. K. Ranghunath, K. P. Rao, and K. T. Joseph, *Biotechnol. Bioeng.,* **26,** 104 (1984).
18. N. A. Peppas, Ed., *Hydrogels In Medicine and Pharmacy,* vol. II, CRC Press, Boca Raton, FL, 1978.
19. J. Kloosterboer, *Adv. Polym. Sci.,* **84,** 1 (1988).
20. H. Boots, J. Kloosterboer, and G. van de Hei, *Br. Polym. J.,* **17,** 219 (1985).
21. J. Bastide and L. Leiber, *Macromolecules,* **22,** 107 (1989).
22. G. P. Simon, P. E. M. Allen, D. J. Bennet, D. R. G. Williams, and E. H. Williams, *Macromolecules,* **22,** 3555 (1989).
23. W. Funke, *Br. Polym. J.,* **21,** 107 (1989).
24. J. Kloosterboer, G. G. Litjen, and H. Boots, *Maromol. Chem. Makromol. Symp.,* **24,** 223 (1989).
25. A. B. Scranton, C. N. Bowman, J. Klier, and N. A. Peppas, *Polymer,* **33,** 1683 (1992).
26. A. Tuncel, K. Ecevit, K. Kesenci, and E. Piskin, *J. Polym. Sci., Part A, Polym. Chem. Ed.,* **34,** 45 (1996).
27. A. Tuncel and E. Piskin, *J. Appl. Polym. Sci.,* **62,** 789 (1996).
28. K. Kesenci, A. Tuncel, and E. Piskin, *Reactive Funct. Polym.,* **31,** 137 (1997).
29. D. S. Clark and J. E. Bailey, *Biotechnol. Bioeng.,* **25,** 1027 (1983).
30. J. M. Guisan, A. Bastida, C. Cuesta, R. F. Lafuente, and C. M. Rossel, *Biotechnol. Bioeng.,* **38,** 1144 (1991).
31. T. Maehara, Y. Eda, K. Mitani, and S. Matsuzawa, *Biomaterials,* **11,** 122 (1990).
32. E. Zurkova, B. D. Zdenkova, Z. Pelzbauer, F. Svec, and J. Kalal, *J. Polym. Sci., Polym. Chem. Ed.,* **21,** 2949 (1983).
33. R. Arshady and A. Ledwith, *Reactive Polym.,* **1,** 159 (1983).
34. A. Mersmann and H. Grossman, *Chem. Eng. Technol.,* **52,** 621 (1980).
35. D. B. Sculles, *J. Appl. Polym. Sci.,* **20,** 2299 (1976).
36. R. C. Weast, Ed., *Handbook of Chemistry and Physics,* 55th ed., CRC Press, Cleveland, 1974.
37. J. Brandup and E. H. Immergut, Eds., *Polymer Handbook,* Wiley Interscience Publishers, Toronto, 1975.
38. R. H. Perry and C. Chilton, Eds., *Chemical Engineers' Handbook,* 5th ed., McGraw Hill Kogakusha Ltd., Tokyo, 1973.